Molecular Determinants of Vanilloid Sensitivity in TRPV1*

**Narender R. Gavva‡§, Lana Klionsky‡, Yusheng Qu‡, Licheng Shi‡, Rami Tamir‡,
Steve Edenson‡, T. J. Zhang‡, Vellarkad N. Viswanadhan¶, Attila Toth‖, Larry V. Pearce‖,
Todd W. Vanderah**, Frank Porreca**, Peter M. Blumberg‖, Jack Lile‡, Yax Sun¶, Ken Wild‡,
Jean-Claude Louis‡, and James J. S. Treanor‡**

*From the Departments of ‡Neuroscience and ¶Molecular Structure, Amgen Inc., Thousand Oaks, California 91320-1799,
the ‖Laboratory of Cellular Carcinogenesis and Tumor Promotion, National Cancer Institute, NIH, Bethesda,
Maryland 20892, and the **Department of Pharmacology, the University of Arizona College of Medicine,
Tucson, Arizona 85724-5017*

Vanilloid receptor 1 (TRPV1), a membrane-associated cation channel, is activated by the pungent vanilloid from chili peppers, capsaicin, and the ultra potent vanilloid from *Euphorbia resinifera*, resiniferatoxin (RTX), as well as by physical stimuli (heat and protons) and proposed endogenous ligands (anandamide, *N*-arachidonyldopamine, *N*-oleoyldopamine, and products of lipoxygenase). Only limited information is available in TRPV1 on the residues that contribute to vanilloid activation. Interestingly, rabbits have been suggested to be insensitive to capsaicin and have been shown to lack detectable [³H]RTX binding in membranes prepared from their dorsal root ganglia. We have cloned rabbit TRPV1 (oTRPV1) and report that it exhibits high homology to rat and human TRPV1. Like its mammalian orthologs, oTRPV1 is selectively expressed in sensory neurons and is sensitive to protons and heat activation but is 100-fold less sensitive to vanilloid activation than either rat or human. Here we identify key residues (Met[547] and Thr[550]) in transmembrane regions 3 and 4 (TM3/4) of rat and human TRPV1 that confer vanilloid sensitivity, [³H]RTX binding and competitive antagonist binding to rabbit TRPV1. We also show that these residues differentially affect ligand recognition as well as the assays of functional response *versus* ligand binding. Furthermore, these residues account for the reported pharmacological differences of RTX, PPAHV (phorbol 12-phenyl-acetate 13-acetate 20-homovanillate) and capsazepine between human and rat TRPV1. Based on our data we propose a model of the TM3/4 region of TRPV1 bound to capsaicin or RTX that may aid in the development of potent TRPV1 antagonists with utility in the treatment of sensory disorders.

The receptor for capsaicin (a small vanilloid molecule extracted from "hot" chili peppers), designated vanilloid receptor 1 (also known as VR1 and TRPV1[1] (1)) has been cloned and shown to be a nonselective cation channel with high permeability to calcium. TRPV1 belongs to a superfamily of ion channels known as transient receptor potential channels (TRPs) several of which appear to be sensors of temperature (2, 3). TRPV1 can be activated by exogenous agonists (capsaicin and RTX) and by physical stimuli such as heat ($>42 °C$) and protons (pH 5). Possible endogenous ligands released during tissue injury have also been suggested, including anandamide (arachidonylethanolamine or AEA) and products of lipoxygenases such as 12-hydroperoxyeicosatetraenoic acid, *N*-arachidonyldopamine (NADA), and *N*-oleoyldopamine (OLDA) (4–7). Ji *et al.* (8) reported that TRPV1 is detectable at increased levels after inflammatory injury in rodents and speculated that the increased level of TRPV1 protein combined with the confluence of stimuli present in inflammatory injury states leads to a reduced threshold of activation of nociceptors that express TRPV1, *i.e.* hyperalgesia. Indeed the converse is true that TRPV1-deficient mice display reduced thermal hypersensitivity following inflammatory tissue injury (9).

Structure-function studies of this channel are in their infancy, but fundamental observations have been reported. Publications of species differences, based upon differential binding of the radiolabeled TRPV1 agonist [³H]RTX to dorsal root ganglia membranes, were recorded even before TRPV1 was cloned (10). Of note, rabbits were found to be resistant to the acute toxicity of capsaicin (11) and were found not to have [³H]RTX binding sites (10). These observations have provided the basis for an approach to identify key regions involved in TRPV1 binding and activation by RTX and capsaicin by cloning TRPV1 from capsaicin-sensitive and insensitive species (rat (1); human (12); rabbit (13, 14); chicken (15); and guinea pig (16)). Rat and human TRPV1 have been pharmacologically characterized proving that capsaicin and RTX are indeed agonists of TRPV1 (capsaicin EC_{50}: 0.05–0.2 μM and RTX EC_{50}: 0.3–11 nM) transiently expressed in HEK293 cells (12, 17–19). Interestingly, these studies have indicated species differences in antagonism, such as the report that capsazepine blocks human but not rat TRPV1 response to low pH (18).

Electrophysiological studies using membrane-impermeable analogues of capsaicin (20) and mutational analysis of extracellular loops (21, 22) have identified domains that contribute to capsaicin and proton activation, respectively. These studies

[1] The abbreviations used are: TRPV1, transient receptor potential vanilloid type 1; RTX, resiniferatoxin; AEA, arachidonyl ethanolamine; NADA, *N*-arachidonyldopamine; OLDA, oleoyldopamine; DRG, dorsal root ganglia; PPAHV, 12-phenylacetate 13-acetate 20-homovanillate; BCTC, *N*-(4-tertiarybutylphenyl)-4-(3-chloropyridin-2-yl)tetrahydropyrazine-1(2H)-carboxamide; CHO, Chinese hamster ovary; BSA, bovine serum albumin; MES, 4-morpholineethanesulfonic acid; r/o, rat-rabbit chimera; h/o, human-rabbit chimera; Iodo-RTX, iodo resiniferatoxin; TM, transmembrane domain.

have demonstrated that capsaicin appears to function from the intracellular side, and protons act on an extracellular site to activate TRPV1. We have previously reported the cloning of rabbit TRPV1 and that it is capsaicin-insensitive but activated by heat (45 °C) and protons (pH 5) in transiently expressed HEK293 cells (13). Jordt and Julius (15) have more recently shown that heterologously expressed chicken TRPV1 (gTRPV1) is similarly insensitive to activation by capsaicin but sensitive to heat (>42 °C) and proton (pH 4.5) stimuli. Furthermore, Jordt and Julius (15) showed that the TM3/4 region of TRPV1 appeared to be responsible for capsaicin sensitivity. Experiments by other investigators have identified additional residues on the N- and C-terminal domains of TRPV1 that also appear to modify capsaicin sensitivity as well as [3H]RTX binding (23, 24).

We describe in the present study amino acids in TRPV1 critical for vanilloid sensitivity by utilizing rabbit TRPV1 (*Oryctolagus cuniculus*, oTRPV1) and selected mutations of the TM3/4 region. We determine, utilizing radioactive calcium ($^{45}Ca^{2+}$) uptake assays and whole cell patch clamp techniques, the sensitivity of oTRPV1 and mutants to the published activators of TRPV1. Binding of [3H]RTX was used to probe residues important for the high affinity binding of this ligand to TRPV1. Furthermore, we examine the functional sensitivity of oTRPV1 and mutants to capsaicin site antagonists and show that gain of capsaicin sensitivity also confers competitive antagonist action at TRPV1. Last, we present a model of capsaicin and RTX bound to the TM3/4 region of rat TRPV1.

EXPERIMENTAL PROCEDURES

Molecular Biology—A cDNA library was made in pSPORT vector from poly(A)+-containing RNA extracted from dorsal root ganglia dissected from New Zealand White rabbits. The library was screened at high stringency (2× SSC, 65 °C) with a rTRPV1 probe (bases 1063–2185, the sequence with GenBank™ accession number AF029310). Several clones were isolated, and the longest full-length clone, designated oTRPV1, was chosen for expression studies. The sequence of this cDNA has been submitted to the GenBank™ (accession number AY487342).

Rat-rabbit (r/o) TRPV1 chimera was generated by restriction cloning. ClaI and PmlI restriction sites were introduced into pcDNA3.1-oTRPV1 construct using QuikChange site-directed mutagenesis kit (Stratagene). Ser505-Thr550 fragment was PCR-amplified from rTRPV1 (ClaI and PmlI sites were included in PCR primers) and cloned into oTRPV1 ClaI-PmlI. Point mutations were introduced using the QuikChange kit following the manufacturer's protocol. All constructs were verified by DNA sequencing.

In Situ Hybridization—In situ hybridization was carried out using 33P-labeled riboprobes as described previously by Wilcox (25). A unique 500-bp PCR fragment of oTRPV1 cDNA was subcloned into the polylinker site of pCR2.1 vector (Invitrogen). Linearized constructs were transcribed with SP6 or T7 RNA polymerase to generate antisense or sense [33P]uridine triphosphate-labeled RNA probes, respectively (Promega SP6/T7 kit). Sections were hybridized overnight at 55 °C with the 33P-labeled antisense or sense riboprobes corresponding to oTRPV1. Sections were examined with dark field and standard illumination (bright field) to allow simultaneous evaluation of tissue morphology and hybridization signal.

Transient Transfections—HEK293 cells were maintained in Dulbecco's modified Eagle's medium (supplemented with 10% fetal bovine serum, penicillin, streptomycin, and L-glutamine). Cells were transiently transfected with a cytomegalovirus promoter-based expression vector (pcDNA3.1, Invitrogen) encoding an appropriate TRPV1 receptor by using FuGENE (Roche Applied Science) transfection reagent (75 μl of FuGENE and 45 μg of plasmid per 1.5–1.7 × 10⁷ cells in a 225-cm² culture flask). After 24 h the large pool of transfected cells was reseeded into Amersham Biosciences Cytostar plates for ^{45}Ca uptake studies, into 3-cm dishes for whole cell patch-clamp recording studies, into clear polystyrene 96-well plates for enzyme-linked immunosorbent assay or immunostaining, or spun down, and pellets were used for [3H]RTX binding assay. Enzyme-linked immunosorbent assay or immunostaining with appropriate anti-VR1 antibodies were used to measure expression levels.

Stable Transfections—CHO cells stably expressing rTRPV1, oTRPV1, oTRPV1-I550T, oTRPV1-L547M, or oTRPV1-L547M/I550T were generated by transfection with pcDNA 3.1-expression vector encoding an appropriate TRPV1 cDNA. Cells were maintained in Dulbecco's modified Eagle's medium supplemented with 10% dialyzed fetal bovine serum, penicillin, streptomycin, L-glutamine, and nonessential amino acids. The CaOPO₄ method was used for stable transfections (5 μg of DNA per 2 × 10⁶ cells in 60-mm dishes). 800 μg/ml Geneticin was used as a selection agent. After about 2 weeks of selection single colonies were picked and screened for expression of TRPV1 in a $^{45}Ca^{2+}$ uptake assay. Positive clones were expanded and used in all of our studies similarly to HEK293 transients.

Functional Assays—The activation of TRPV1 is followed as a function of cellular uptake of radioactive calcium ($^{45}Ca^{2+}$, ICN). All the $^{45}Ca^{2+}$ uptake assays had a final $^{45}Ca^{2+}$ at 10 μCi/ml. The assays were as follows: 1) Agonist assay: agonists were incubated with vector or TRPV1 expressing HEK293 cells in 1:1 ratio of F-12 and Hanks' buffered saline solution supplemented with BSA, 0.1 mg/ml, and 1 mM HEPES at pH 7.4 at room temperature for 2 min in the presence of $^{45}Ca^{2+}$ prior to compound washout. 2) Capsaicin antagonist assay: compounds were preincubated with vector or TRPV1 expressing HEK293 or CHO cells in Hanks' buffered saline solution supplemented with BSA, 0.1 mg/ml, and 1 mM HEPES at pH 7.4 at room temperature for 2 min prior to addition of $^{45}Ca^{2+}$ in F-12 and then left for an additional 2 min prior to compound washout. 3) Proton antagonist assay: compounds were preincubated with vector or TRPV1 expressing HEK293 or CHO cells at room temperature for 2 min prior to addition of $^{45}Ca^{2+}$ in 30 mM HEPES/MES buffer (final assay pH 5) and then left for an additional 2 min prior to compound washout. 4) Compound washout and analysis: assay plates were washed two times with phosphate-buffered saline, 0.1 mg/ml BSA using an ELX405 plate washer (Bio-Tek Instruments Inc.) immediately after functional assay. Radioactivity in the 96-well plates was measured using a MicroBeta Jet (Wallac Inc.). Compound activity was then calculated using GraphPad Prism. Maximum $^{45}Ca^{2+}$ uptake in agonist dose response was considered as 100% for each agonist in calculating the EC_{50} values.

[3H]RTX Binding Assay—Binding studies with [3H]RTX were carried as described previously with minor modifications (10). Binding assay mixtures were set up on ice in glass tubes (Kimble Glass Inc.) and consisted of 200 μl of binding buffer (5 mM KCl, 5.8 mM NaCl, 0.75 mM CaCl₂, 2 mM MgCl₂, 137 mM sucrose, 10 mM HEPES, pH 7.8), 50 μl of [3H]RTX (different concentrations, 37 Ci/mmol specific activity, PerkinElmer Life Sciences) and 100 μl of cell suspension (0.5–1 × 10⁶/per tube). The assay mix contained BSA at a final concentration of 0.25 mg/ml (Cohn fraction V, Sigma). In each set of experiments, total binding and nonspecific binding were defined in the presence of 3.5 μl of cold RTX (1 μM final concentration). The reaction mixtures were incubated at 37 °C shaking water bath for 1 h (50 rpm). Binding reactions were terminated by chilling the assay mixtures on ice for 5 min. 100 μl of α_1-acid glycoprotein (2 mg/ml; Sigma) was added into the binding mix and incubated for an additional 10 min to reduce nonspecific binding. The bound and free ligands were separated by centrifugation in a Beckman 12 Microfuge. The tip of the Microfuge tubes containing the cell pellet was cut off, and the bound radioactivity was determined by scintillation counting (Wallac). Data was analyzed using GraphPad Prism.

Electrophysiology—HEK293 cells transiently expressing the TRPV1 channels were maintained at 37 °C in a 5% CO_2 atmosphere. Whole-cell membrane currents were recorded using the whole cell patch-clamp technique (26). The external calcium-free recording solution contained 140 mM NaCl, 5 mM KCl, 10 mM EGTA, 2 mM MgCl₂, 10 mM HEPES, and 10 mM glucose, pH 7.4. Recording micropipettes were filled with an internal recording solution containing 140 mM CsCl, 10 mM EGTA, and 10 mM HEPES, pH 7.2. The micropipettes had resistances ranging from 2 to 4 mΩ and were connected to an AxoPatch 200B patch-clamp amplifier (Axon Instruments Inc.), driven by a desktop computer through a DigiData 1322A digitizer (Axon Instruments Inc.). Liquid junction potentials were manually corrected before establishing the seal. Upon achieving a GΩ seal, the patch was ruptured and whole cell currents were recorded during the application of voltage pulses generated using pClamp version 8.0 software (Axon Instruments Inc.). Currents were filtered at 5 kHz by a low pass 8-pole Bessel filter and acquired at 10 kHz, in episodic mode. All experiments were conducted at room temperature (20–22 °C) by holding the membrane potential at −60 mV. A "sewer-pipe" perfusion system (Rapid Solution Changer model RSC-200, Bio-Logic Science Instrument SA, France) was used to apply solutions directly to the cell under study. Capsaicin and Ruthenium Red were dissolved directly into external recording solution. Re-

TABLE I
*Identity and homology between TRPV1 from different species
(rabbit, oTRPV1; rat, rTRPV1; human, hTRPV1; chicken, gTRPV1;
guinea pig, gpTRPV1)*

For each species identity is shown at the top, and similarity is shown in the bottom row.

	oTRPV1	hTRPV1	gpTRPV1	gTRPV1
		%		
rTRPV1	86	85	85	65
	91	92	91	77
oTRPV1		87	84	65
		92	90	77
hTRPV1			84	64
			90	77
gpTRPV1				64
				76

cording solutions were adjusted to the desired pH by adding HCl. Data was analyzed using pClamp version 8.0 and Prism version 3.02 (GraphPad).

Molecular Modeling—Molecular modeling was carried out using Insight II (2000) software (Accelrys Inc.). Transmembrane helices and connecting segments were modeled using the Biopolymer module of Insight II (2000). RTX and capsaicin structures were generated and minimized using Insight II tools.

RESULTS

All studies of mutant TRPV1 function were conducted using transient transfections in HEK293 cells. Transient transfections of HEK293 cells followed by immunohistochemical staining for TRPV1 protein indicated that all TRPV1 cDNAs studied in this report appeared to be expressed. However, this technique did not allow for quantitative analysis of the number of functional channels expressed on the cell surface, and as such all of the data presented here are discussed as relative activity. Interpretation of $^{45}Ca^{2+}$ uptake assays utilizing different TRPV1 mutants assumed that all have the same permeability to calcium ions. oTRPV1 gain-of-function mutants were also characterized by stable expression in CHO cells.

oTRPV1 Is Less Sensitive to Capsaicin Activation Than Rat TRPV1—To determine if oTRPV1 is indeed less sensitive to vanilloids than other species, oTRPV1 was cloned from a bacterial colony screen of a rabbit DRG cDNA library utilizing hybridization with a radiolabeled ^{32}P-rTRPV1 probe. A cDNA clone (2.4 kb) was identified whose predicted protein sequence had high homology to rTRPV1 (86% identity and 91% similarity) and hTRPV1 (87% identity and 92% similarity; Table I and Fig. 1A). *In situ* hybridization of rabbit dorsal root ganglia (DRG) sections with a probe generated from the oTRPV1 cDNA revealed strong labeling of cells in the DRG (Fig. 1B) with expression restricted to the small and medium diameter cell bodies consistent with that seen in other species. Studies showed that conditions capable of robustly activating rTRPV1 had a mixed effect on oTRPV1. Whereas oTRPV1 was activated by heat (45 °C) or pH 5 similar to rTRPV1, it was not activated by capsaicin at supra-maximal activation concentrations for rTRPV1 (Fig. 1C). Furthermore, oTRPV1-transfected HEK293 cells did not show any specific [^{3}H]RTX binding, whereas rTRPV1-transfected cells showed specific binding with a K_D value of 0.089 ± 0.01 nM.

Agonist sensitivity was also characterized by electrophysiology. Perfusion of voltage-clamped cells transiently expressing TRPV1 with low pH solution elicited an inward current, with amplitudes that increased with lower pH (*e.g.* Fig. 1D). Average peak currents at pH 5 for rTRPV1 and oTRPV1 were 310.3 ± 85.8 µA/microfarad (*n* = 5), 281.9 ± 24.6 µA/microfarad (*n* = 5), respectively. Low pH elicited a much smaller current of 1.02 ± 0.93 pA/picofarad (*n* = 6 cells) in mock transfected HEK293 cells, which indicated that the proton-

activated current in (rat and rabbit) TRPV1-transfected cells was primarily mediated by TRPV1. Large currents were also observed in response to 1 and 10 µM capsaicin in rTRPV1-transfected cells. In contrast, 1 µM capsaicin failed to generate any current in oTRPV1-transfected cells, although 10 µM evoked a small current (Fig. 1D). These experiments confirmed that oTRPV1 was functionally expressed in HEK293 cells and that oTRPV1 was much less sensitive to activation by capsaicin than rTRPV1. However, the small current elicited with 10 µM capsaicin suggested a rudimentary capsaicin-site in oTRPV1. The ability of Ruthenium Red to block oTRPV1 was also tested in patch-clamp studies. Ruthenium Red (10 µM) application 10 s after pH 5 activation blocked 83.4 ± 8.2% of the oTRPV1 current (*n* = 5 cells; Fig. 1E). These data verified that proton activation of oTRPV1 is sensitive to pore blockade similar to rTRPV1. In summary, sequence similarities to TRPV1s from other species, the activation profile of oTRPV1 by proton and heat, blockade of the proton and heat responses by Ruthenium Red, and the expression pattern of oTRPV1 mRNA in rabbit dorsal root ganglia confirm that oTRPV1 is the rabbit orthologue of TRPV1. The limited sensitivity of oTRPV1 to capsaicin and RTX and lack of detectable [^{3}H]RTX binding agree with published data on the expected properties of oTRPV1 (10, 11).

Residue 550 Is an Important Determinant for Vanilloid Sensitivity in oTRPV1—A rat-rabbit chimera (r/o chimera) of TRPV1 was constructed by transfer of transmembrane domains 3 through 4 (amino acids Ser^{505}-Thr^{550}) from rTRPV1 to oTRPV1, because Jordt and Julius (15) previously showed that the TM3/4 region of TRPV1 appears to be responsible for capsaicin sensitivity. Functional analysis of transiently transfected cells by $^{45}Ca^{2+}$ uptake showed that the r/o chimera gained sensitivity to vanilloids (EC$_{50}$ for capsaicin: 0.051 ± 0.029 µM and RTX: 11 ± 5 nM) similar to rTRPV1 (Fig. 2A). Sensitivity of the r/o chimera to capsaicin was also characterized by electrophysiology. Currents evoked by pH 5 and 1 µM capsaicin were similar in the chimera and rTRPV1 (Figs. 1D and 2A, *bottom panel*). In addition, we also made a human-rabbit chimera (h/o chimera) transferring the Ser^{505}-Thr^{550} from hTRPV1 to oTRPV1. Similar to r/o chimera, functional analysis showed that h/o chimera gained sensitivity to capsaicin (Fig. 2A), further confirming that the TM3/4 region is responsible for vanilloid sensitivity.

Amino acid sequence alignment of the 505–550 region indicated that ten amino acids are different between rat and rabbit TRPV1, and six amino acids are different between human and rabbit TRPV1 (Fig. 2C). To determine which residues within this region were responsible for gain of functional sensitivity to vanilloids in oTRPV1, we mutated the residues that are different in rabbit from both rat and human TRPV1 (A505S, A520S, C534R, T540S, and I550T). Remarkably, changing the single residue at 550 in rabbit to the corresponding residue found in rat and human TRPV1 (I550T) was sufficient to confer gain of function for activation by capsaicin (Fig. 2B). Dose-response curves in $^{45}Ca^{2+}$-uptake experiments indicated that the EC$_{50}$ of capsaicin at the oTRPV1 channel was 14.8 ± 7.9 µM, whereas it was 0.016 ± 0.006 µM for rTRPV1, 0.051 ± 0.029 µM for the r/o chimera (described above), and 0.052 ± 0.034 µM for oTRPV1-I550T. In addition to the above studies using transiently transfected HEK293 cells, we have also verified oTRPV1-I550T sensitivity to vanilloids in stably expressing CHO cells. Vector-transfected HEK293 or parental CHO cells did not show significant $^{45}Ca^{2+}$-uptake up to 40 µM capsaicin or 10 µM RTX. Other known TRPV1 agonists (Arvanil, Olvanil, 12-phenylacetate 13-acetate 20-homovanillate (PPAHV), NADA, and OLDA) were inactive up to 40 µM at wild type oTRPV1 but functioned as potent agonists at oTRPV1-I550T
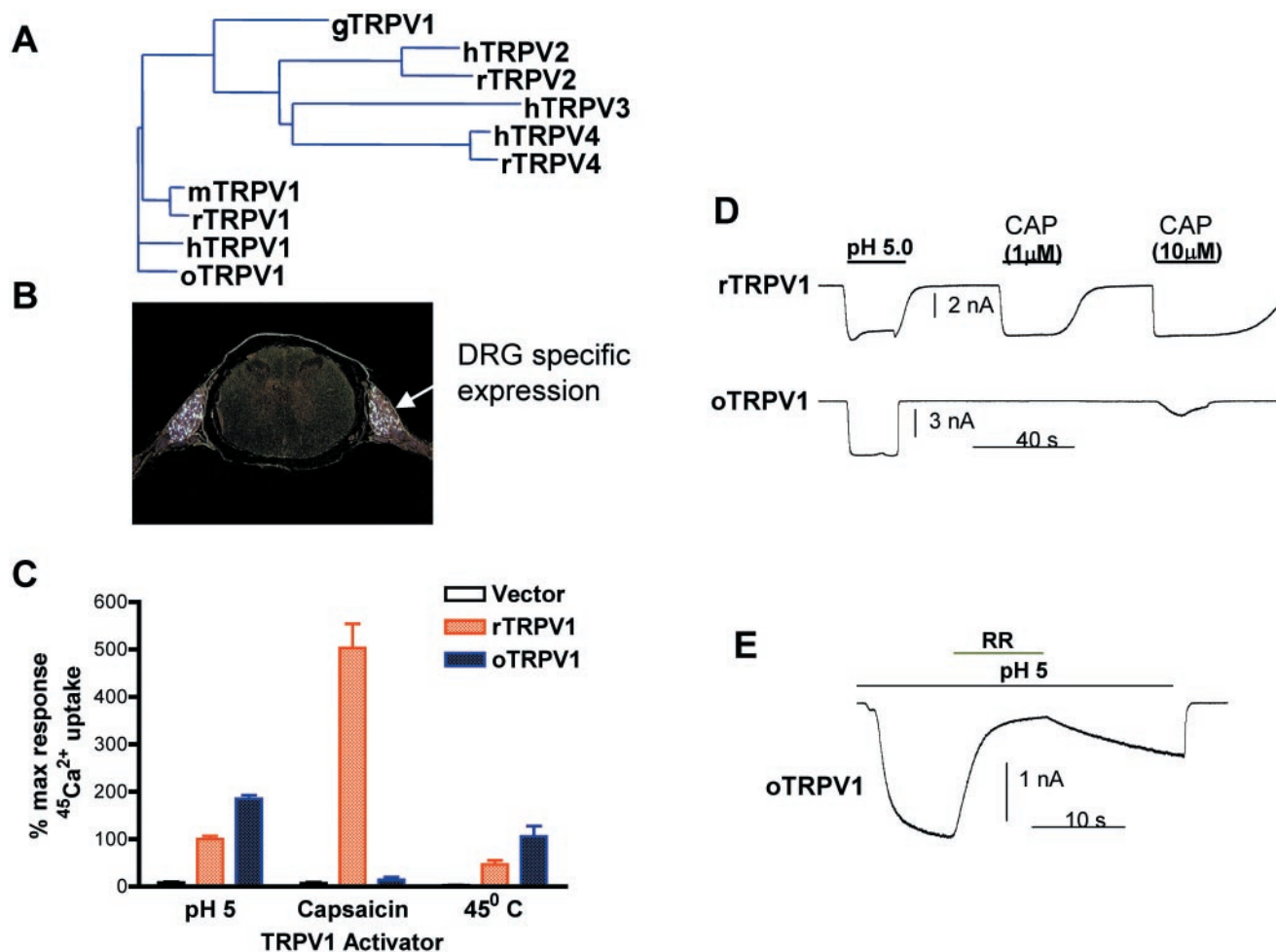
FIG. 1. **Rabbit TRPV1 (oTRPV1) responds to heat or protons, but is less sensitive to capsaicin.** *A*, phylogenetic tree based on ClustalW alignment of TRPV1 and related TRPV protein sequences. *B, in situ* hybridization showing dorsal root ganglia-enriched expression of TRPV1 in rabbit. *C*, activation of $^{45}Ca^{2+}$ uptake in HEK293 cells transiently expressing rat or rabbit TRPV1 with protons (pH 5), capsaicin (0.5 μM), or heat (45 °C). Responses of HEK293 cells transfected with an expression vector alone are included. Results are shown as mean ± S.D. from three independent experiments, each performed in triplicate. Proton (pH 5)-induced $^{45}Ca^{2+}$ uptake in rat TRPV1-expressing HEK293 cells was considered 100%, and all data are shown as relative percentages. *D*, patch clamp electrophysiology was used to examine rabbit and rat TRPV1 by transient expression in HEK293 cells. Average peak currents at pH 5 for rat and rabbit TRPV1 were 310.3 ± 85.8 μA/microfarad (μF) (n = 5), 281.9 ± 24.6 μA/μF (n = 5), respectively. Subsequent perfusion with capsaicin (1 μM) produced no detectable current, and 10 μM produced very small current in oTRPV1-expressing cells; in contrast, rat TRPV1 was robustly activated by both concentrations of capsaicin. *E*, Ruthenium Red block of proton-evoked currents in oTRPV1-expressing HEK293 cells. The pH of the extracellular solution was lowered from 7.2 to 5 for 10 s. At the second application, Ruthenium Red (10 μM) was co-applied for 10 s while the extracellular solution was held at pH 5. The average block of proton-activated currents after 10 s was 83.4 ± 8.2% (n = 5).

(Table II). Changing residues A505S, A520S, C534R, and T540S individually or in various combinations did not cause any changes in response of oTRPV1 to vanilloids (data not shown). Lastly, patch clamp recordings confirmed gain of capsaicin sensitivity in oTRPV1-I550T; currents evoked by pH 5, 1, or 10 μM capsaicin were similar in r/o chimera and oTRPV1-I550T-transfected cells indicating that indeed Thr[550] confers vanilloid sensitivity (Fig. 2, *A* and *B*).

To better understand the biophysical requirements at position 550, we explored several polar and hydrophobic substitutions. A similar gain in capsaicin sensitivity was observed when a serine instead of threonine residue was introduced at position 550 (I550S) of oTRPV1 (EC_{50} value: 0.11 ± 0.07 μM). However, replacement of the hydroxyl group-bearing residue at this position with the small nonpolar alanine only resulted in partial gain of capsaicin sensitivity (EC_{50} value: 0.81 ± 0.67 μM) and substitution with the thiol group containing residue cysteine resulted in a very small gain in oTRPV1 capsaicin sensitivity (EC_{50} value: 2.1 ± 0.6 μM). Although capsaicin sensitivity of I550T, I550S, I550A, and I550C oTRPV1 mutants varied, their responses to proton activation remained similar to

wild type oTRPV1 (data not shown). Introduction of tyrosine with its bulky phenolic side chain at this position resulted in a complete loss of TRPV1 response to vanilloid, proton, or heat activation, although expression levels of this mutant remained comparable to others (data not shown).

Thr[550] Is an Important Determinant for Vanilloid Sensitivity in Rat and Human TRPV1—To further verify that the Thr[550] found in native rat and human TRPV1 contributes to vanilloid sensitivity of TRPV1, we conducted a loss of function study by substituting the natural threonine with the oTRPV1 isoleucine-550 residue. Dose-response curves in $^{45}Ca^{2+}$-uptake experiments demonstrated that the EC_{50} of capsaicin at the mutant rTRPV1-T550I is shifted to 0.608 ± 0.032 μM from 0.057 ± 0.014 μM at wild type rTRPV1 channel, about a 10-fold loss in sensitivity (Fig. 3*A*). EC_{50} of capsaicin at the mutant hTRPV1-T550I is shifted to 4.58 ± 0.6 μM from 0.12 ± 0.05 μM at wild type hTRPV1 channel, approximately a 40-fold loss in sensitivity (Fig. 3*A*). Patch clamp recordings also confirmed loss of capsaicin sensitivity in rTRPV1-T550I and hTRPV1-T550I; 1 μM capsaicin failed to generate any current in TRPV1-T550I-transfected cells, although 10 μM did evoke currents (Fig. 3*B*).
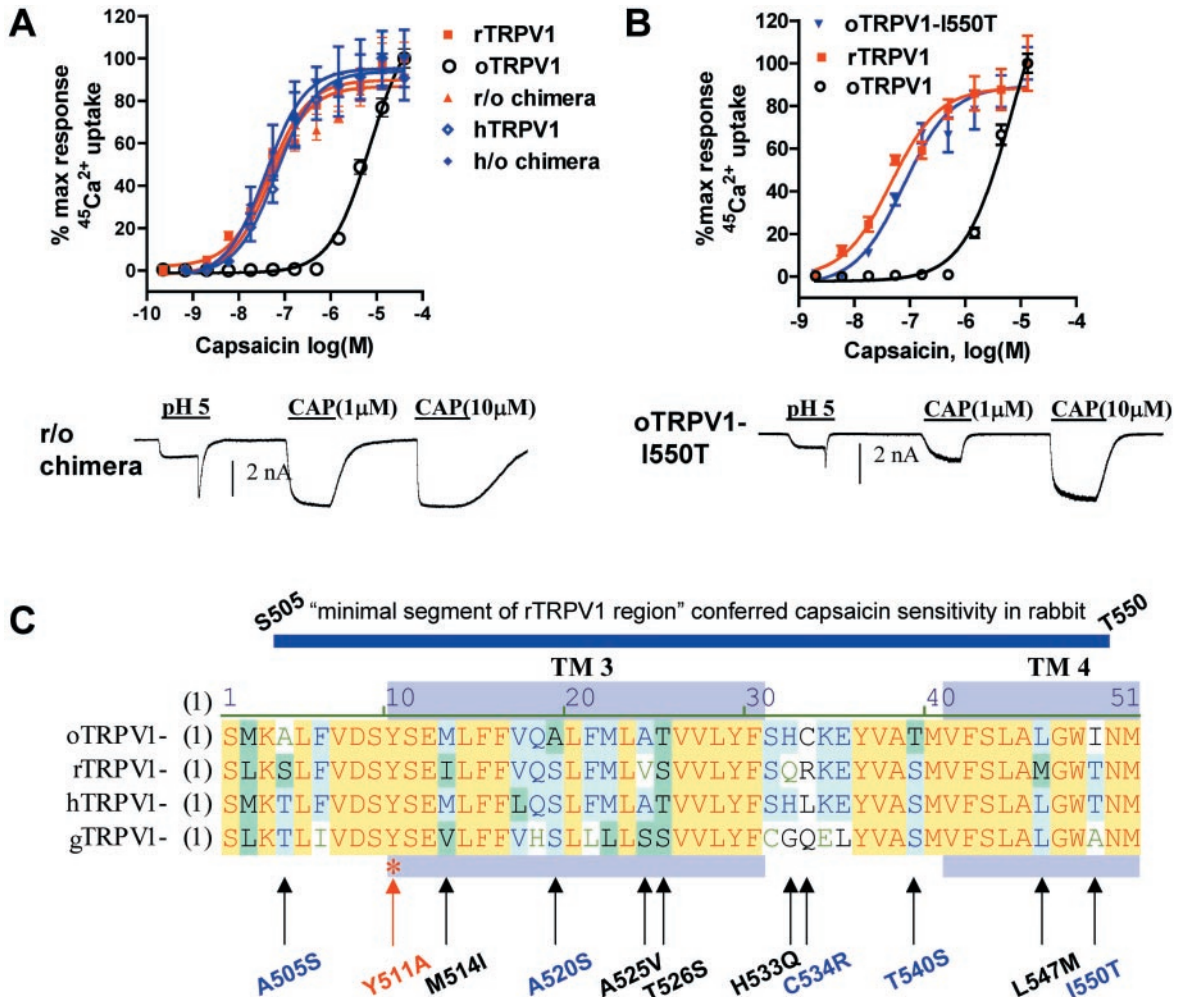
FIG. 2. **Substitution of the Ser[505]-Thr[550] region or I550T alone confer capsaicin sensitivity to oTRPV1.** *A*, *top panel*: concentration-dependent capsaicin-induced $^{45}Ca^{2+}$ uptake by HEK293 cells transiently transfected with expression plasmids encoding rat, rabbit, rat/rabbit (r/o) chimera, human, or human/rabbit (h/o) TRPV1 chimera. TRPV1 r/o chimera shows sensitivity to capsaicin similar to rTRPV1 (EC_{50} values of 0.051 ± 0.029 μM and 0.046 ± 0.036 μM, respectively). TRPV1 h/o chimera shows sensitivity to capsaicin similar to hTRPV1. (EC_{50} values of 0.048 ± 0.019 μM and 0.072 ± 0.029 μM, respectively). Similar results were obtained in six independent experiments; *error bars* indicate S.E. *Bottom panel*: proton and capsaicin-evoked currents in HEK293 cells transfected with TRPV1 r/o chimera. Capsaicin (1 or 10 μM) response of r/o chimera is similar to that of rTRPV1. *B*, *top panel*: stimulation of $^{45}Ca^{2+}$ uptake into HEK293 cells transiently transfected with rat, rabbit, or rabbit I550T mutant of TRPV1 by capsaicin. I550T mutation alone confers capsaicin sensitivity to oTRPV1 (EC_{50} value: 0.052 ± 0.034 μM ($n = 12$), similar to that of rat TRPV1). *Bottom panel*: representative current trace recorded from HEK293 cells expressing oTRPV1-I550T demonstrate gain of capsaicin sensitivity compared with oTRPV1. *C*, sequence alignment of rabbit (*o*), rat (*r*), human (*h*), and chicken (*g*) TRPV1 within TM3–TM4 region is shown. Within the Ser[505]-Thr[550] region (indicated at the *top*), ten amino acids are different between rat and rabbit TRPV1, and six amino acids are different between human and rabbit TRPV1. The mutations generated in oTRPV1 are indicated at the *bottom*. Mutations made at the residues that are different in oTRPV1 from both rat and human are indicated by *blue*. The Y511A mutation that is conserved in all species is shown in *red*.

TABLE II
Comparison of agonist activation of TRPV1 and mutants

Selected agonists were tested in CHO cells stably expressing rTRPV1, oTRPV1, oTRPV1-L547M, oTRPV1-I550T, or oTRPV1-L547M/I550T. EC_{50} value for each cell line was determined using Prism software and expressed in micromolar. The quantitative comparison of the calcium responses to RTX and to capsaicin is complicated by technical issues that should be noted. In particular, the time course of response to RTX is slow compared to that for capsaicin. Under our conditions of a 2-min exposure to drug, therefore, the potency of RTX may be underestimated slightly relative to capsaicin, although it should not invalidate the comparison of relative potencies for the different TRPV1 mutants.

	oTRPV1	oTRPV1-L547M	oTRPV1-I550T	oTRPV1-L547M/I550T	rTRPV1	hTRPV1
Capsaicin	14.832 ± 7.919	8.168 ± 0.624	0.052 ± 0.034	0.021 ± 0.010	0.016 ± 0.006	0.038 ± 0.019
RTX	0.655 ± 0.050	0.021 ± 0.002	0.011 ± 0.005	0.002 ± 0.001	0.003 ± 0.001	0.005 ± 0.002
PPAHV	>40	>40	>40	0.037 ± 0.015	0.034 ± 0.005	15.5 ± 10
Arvanil	>40	>40	0.049 ± 0.017	0.017 ± 0.008	0.019 ± 0.009	0.145 ± 0.037
Olvanil	>40	>40	0.019 ± 0.008	0.011 ± 0.007	0.012 ± 0.005	0.056 ± 0.021
OLDA	>40	>40	7.269 ± 1.737	7.597 ± 1.694	3.915 ± 0.403	15.6 ± 6
NADA	>40	>40	6.105 ± 2.197	5.626 ± 0.596	3.480 ± 0.361	4.5 ± 0.4

Protons (pH 5) still evoked large currents in TRPV1-T550I-transfected cells indicating that only capsaicin sensitivity was reduced. Gain of vanilloid sensitivity with I550T mutation in oTRPV1 and loss with a reverse mutation in rat and human TRPV1-T550I strongly suggests that Thr[550] is one of the critical molecular determinants for TRPV1 activation by vanilloids.
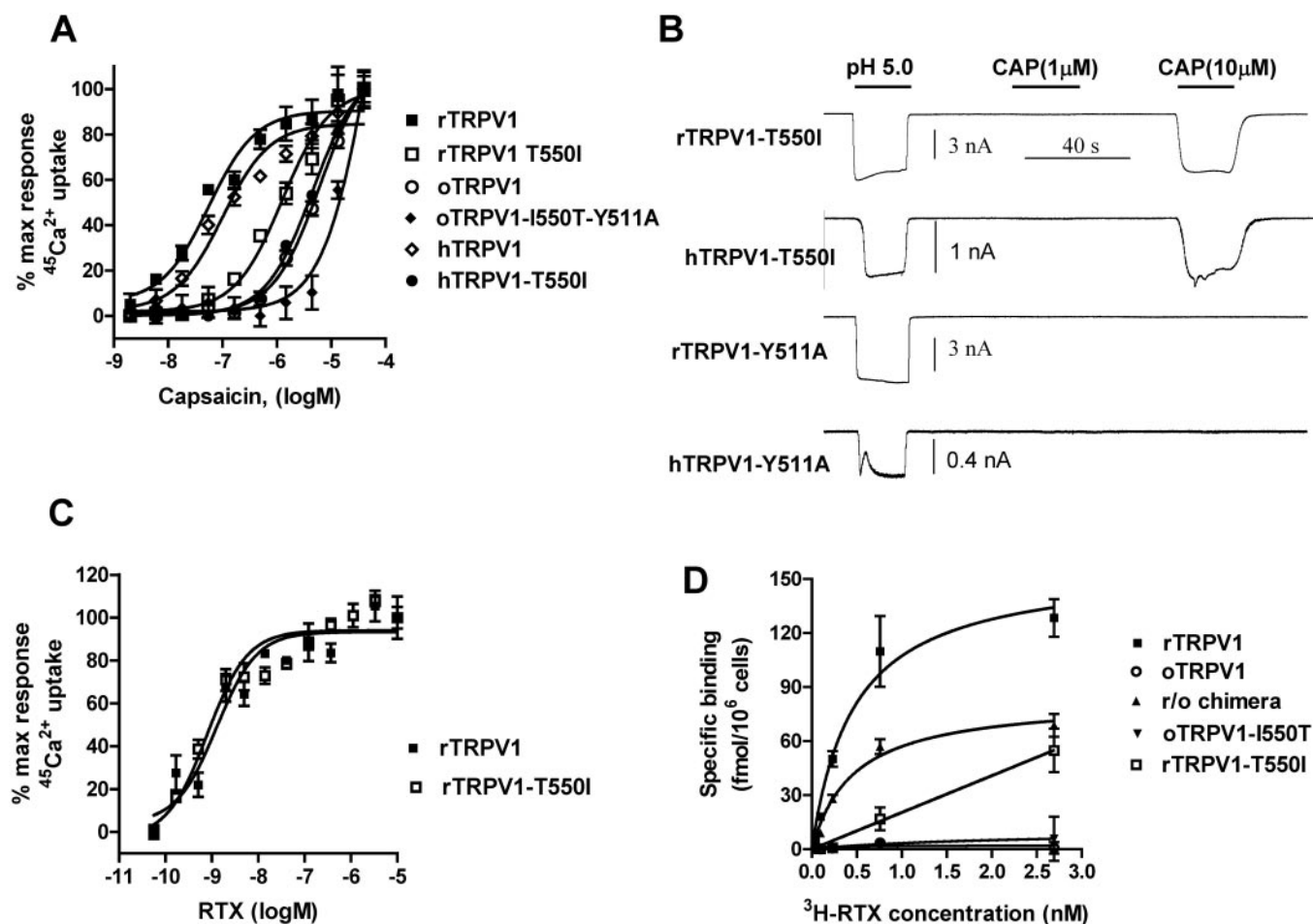
FIG. 3. **Residues Thr[550] and Tyr[511] are critical for vanilloid sensitivity of TRPV1.** *A*, representative concentration-response curves of capsaicin-induced $^{45}Ca^{2+}$ uptake by HEK293 cells expressing rTRPV1, rTRPV1-T550I, oTRPV1, oTRPV1-I550T/Y511A, hTRPV1, or hTRPV1-T550I. Mutation of T550I caused a 10-fold reduction in rTRPV1 capsaicin sensitivity (EC_{50} value for rTRPV1-T550I is 0.608 ± 0.032 μM and for rTRPV1 it is 0.057 ± 0.014 μM, $n = 12$). Note the similar rightward shift in capsaicin dose response for hTRPV1-T550I compared with hTRPV1. Similar results were observed in three independent experiments. *B*, representative current traces from HEK293 cells expressing rTRPV1-T550I, rTRPV1-Y511A, hTRPV1-T550I, or hTRPV1-Y511A demonstrate a loss of sensitivity to capsaicin but not extracellular protons (pH 5). *C*, stimulation of $^{45}Ca^{2+}$ uptake into rTRPV1 or rTRPV1-T550I mutant-expressing HEK293 cells by RTX. EC_{50} values are 1.5 ± 1.06 nM ($n = 4$) for wild type rTRPV1 and 0.93 ± 0.69 nM ($n = 4$) for the rTRPV1-T550I mutant. Similar results were obtained in repeated experiments; *error bars* represent S.E. *D*, specific binding of [^{3}H]RTX to HEK293 cells expressing rat, rabbit, rat/rabbit (r/o) chimera, oTRPV1-I550T, or rTRPV1-T550I mutants. Wild type rTRPV1 and r/o chimera showed saturable-specific [^{3}H]RTX binding, whereas the wild type rabbit TRPV1 and oTRPV1-I550T did not. rTRPV1-T550I shows significant loss in specific [^{3}H]RTX binding. K_D values for rTRPV1 and (r/o) chimera are 0.089 ± 0.01 and 0.07 ± 0.03 nM, respectively.

Based on their mutational data, Jordt and Julius (15) reported that Tyr[511] is critical for vanilloid sensitivity. Tyr[511] is conserved in TRPV1 from all species reported to date. We have verified that the Tyr[511] is critical for vanilloid sensitivity; rTRPV1-Y511A and hTRPV1-Y511A lost vanilloid sensitivity as shown by electrophysiology (Fig. 3*B*). In contrast to rTRPV1, 1 or 10 μM capsaicin failed to elicit any current, whereas pH 5-evoked currents were similar to rTRPV1 (Figs. 1*D* and 3*B*). In addition, we have tested capsaicin sensitivity of oTRPV1 double mutant containing I550T (gain of function) and Y511A (loss of function), *i.e.* oTRPV1-Y511A/I550T. Compared with oTRPV1-I550T, the reduction in capsaicin sensitivity of oTRPV1-Y511A/I550T in $^{45}Ca^{2+}$ uptake assay is >100-fold. In fact the magnitude in loss of capsaicin sensitivity by Y511A is greater than the gain seen in I550T as represented by the rightward shift of the oTRPV1-Y511A/I550T capsaicin dose-response curve beyond the wild type oTRPV1 (Fig. 3*A*). These studies confirm that Tyr[511] is indeed an important molecular determinant for vanilloid sensitivity of TRPV1.

Interestingly, mutation of rat Thr[550] to the corresponding rabbit Ile[550] (T550I) resulted in the capsaicin dose-response curve shifting 10-fold to the right, whereas it did not appear to reduce RTX sensitivity in the $^{45}Ca^{2+}$ uptake assay (EC_{50} values for rTRPV1 and rTRPV1-T550I are 1.5 ± 1.06 nM and 0.93 ± 0.69 nM, respectively; Fig. 3*C*). However, [^{3}H]RTX specific binding was significantly reduced in rTRPV1-T550I-transfected cells (Fig. 3*D*). For the first time, we report a difference in the molecular determinants for the functional responses of TRPV1 to capsaicin and RTX. In oTRPV1, which is an insensitive species, replacement of Ile[550] with Thr[550] contributes to both capsaicin and RTX sensitivity (functional responses), whereas replacement of Thr[550] in rat TRPV1 with an amino acid present in rabbit TRPV1 (Ile[550]) results in partial loss of functional response to the low affinity agonist, capsaicin, but not to the high affinity agonist, RTX.

Functional and binding properties of oTRPV1-I550T were characterized utilizing HEK293 cells transiently transfected or CHO cells stably transfected with the oTRPV1-I550T expression plasmid. Although both cell lines demonstrated a robust functional response ($^{45}Ca^{2+}$ uptake) to proton and vanilloid activation (Fig. 2*B* and data not shown), the same oTRPV1-I550T-expressing cells failed to show any measurable [^{3}H]RTX specific binding. In contrast, the oTRPV1 chimera (r/o chimera) containing the entire rat Ser[505]-Thr[550] region showed specific
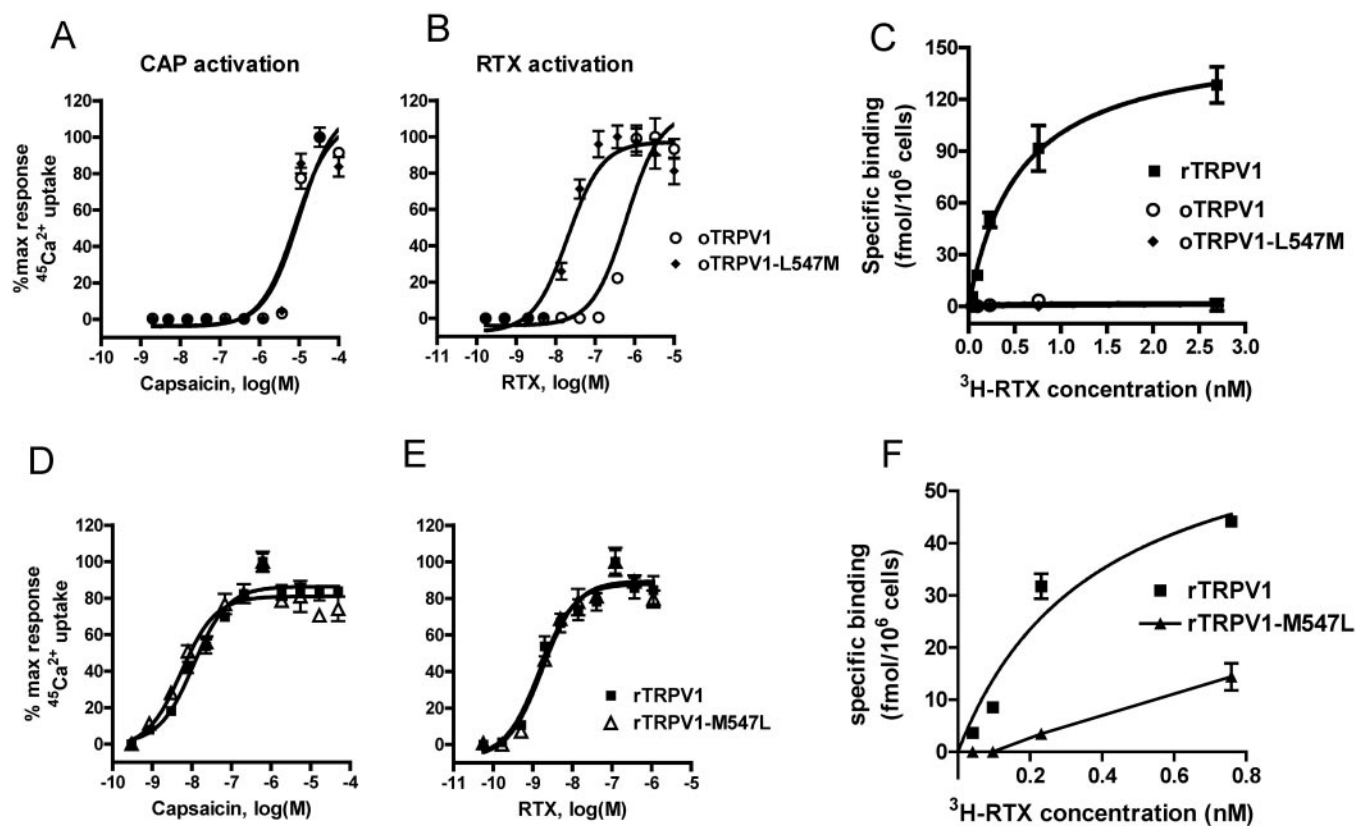
FIG. 4. **Met[547] selectively contributes to RTX sensitivity of TRPV1.** HEK293 cells transiently transfected with oTRPV1, oTRPV1-L547M, rTRPV1, or rTRPV1-M547L were used in $^{45}Ca^{2+}$ uptake and [^{3}H]RTX binding. Each experiment was repeated twice; *error bars* represent S.E. Stimulation of $^{45}Ca^{2+}$ uptake into HEK293 cells expressing oTRPV1 or oTRPV1-L547M by capsaicin (*A*) or RTX (*B*) show a selective 30-fold gain in sensitivity to RTX by the oTRPV1-L547M mutant. EC_{50} values are $0.655 \pm 0.050 \ \mu M$ ($n = 4$) and $0.021 \pm 0.002 \ \mu M$ ($n = 4$) for oTRPV1 and oTRPV1-L547M, respectively. However, there was no specific [^{3}H]RTX binding to cells expressing oTRPV1-L547M (*C*). Stimulation of $^{45}Ca^{2+}$ uptake into HEK293 cells expressing rTRPV1 or rTRPV1-M547L by capsaicin (*D*) or RTX (*E*) show no change in capsaicin or RTX sensitivity. Capsaicin EC_{50} values are $0.011 \pm 0.002 \ \mu M$ ($n = 4$) and $0.009 \pm 0.002 \ \mu M$ ($n = 4$) for rTRPV1 and rTRPV1-M547L, respectively. RTX EC_{50} values are 1.5 ± 0.7 nM ($n = 4$) and 1.7 ± 0.8 nM ($n = 4$) for rTRPV1 and rTRPV1-M547L, respectively. However, specific binding of [^{3}H]RTX to HEK293 cells expressing rTRPV1-M547L shows a significant loss compared with rTRPV1 (*F*).

binding with a K_D value of 0.07 ± 0.03 nM (Fig. 3*D*). These results led us to believe that additional residues within the Ser[505]-Thr[550] region were necessary to attain measurable [^{3}H]RTX binding in oTRPV1.

Discrepancy between RTX responses in functional and binding assays has been reported previously (27, 28). As discussed elsewhere in detail (29), an emerging plausible explanation is that most of the TRPV1 is internal and only a small proportion is localized to the plasma membrane. The minor subpopulation of TRPV1 at the plasma membrane mediates the $^{45}Ca^{2+}$ uptake measurements, whereas the binding analysis is dominated by the predominant, internal TRPV1, and these two populations of TRPV1 display different structure-activity relations, presumably reflecting differential modification. Our results described here demonstrate differences in the receptor requirements for RTX in these two assays and suggest the importance of additional residues in TRPV1 affinity for [^{3}H]RTX. Consequently, to explore the remaining residues that are different between rat and rabbit, we introduced a series of single point mutations into oTRPV1 (M514I, A525V, T526S, H533Q, and L547M) to mimic the residues in rat TRPV1, which has been shown to display the highest RTX binding affinity.

Met[547] in TRPV1 Contributes to RTX Affinity as Detected by Ligand Binding—Replacement of oTRPV1 residues individually at Met[514], Ala[525], Thr[526], and His[533] to corresponding residues in rTRPV1 (M514I, A525V, T526S, and H533Q) did not alter the oTRPV1 response to capsaicin or RTX (data not shown). Interestingly, the single residue change L547M in

oTRPV1 resulted in a selective gain of ~30-fold higher sensitivity to RTX with no apparent change in capsaicin sensitivity in $^{45}Ca^{2+}$-uptake assays (Fig. 4, *A* and *B*). EC_{50} values at oTRPV1 and oTRPV1-L547M were 655 ± 50 nM and 21 ± 2 nM for RTX and $10.1 \pm 2.34 \ \mu M$ and $8.2 \pm 0.6 \ \mu M$ for capsaicin, respectively (Table II). This indicates that Met[547] is one of the critical residues contributing to RTX sensitivity. Although oTRPV1-L547M gained sensitivity to RTX in both transiently transfected HEK293 and stably expressed CHO cells, this mutant failed to show any measurable [^{3}H]RTX binding (Fig. 4*C*). We hypothesized that L547M contributes to RTX sensitivity but requires additional residues such as Thr[550] for sufficient affinity needed for measurable [^{3}H]RTX binding above the assay background.

To investigate whether Met[547] contributes to RTX affinity in rTRPV1, a reverse mutation was made (M547L). Wild type rTRPV1 and rTRPV1-M547L showed similar responses to capsaicin and RTX in the functional $^{45}Ca^{2+}$-uptake assay (Fig. 4, *D* and *E*); EC_{50} values at rTRPV1 and rTRPV1-M547L were 1.5 ± 0.7 nM and 1.7 ± 0.8 nM for RTX and $0.013 \pm 0.002 \ \mu M$ and $0.012 \pm 0.002 \ \mu M$ for capsaicin, respectively. However, the rTRPV1-M547L mutant showed significantly reduced [^{3}H]RTX binding compared with wild type rTRPV1, demonstrating a discrepancy between functional assays and binding once again (Fig. 4*F*) and indicates that Met[547] indeed contributes to RTX affinity in the binding assays.

Both Met[547] and Thr[550] Are Required for Measurable [^{3}H]RTX Binding in oTRPV1—The oTRPV1-L547M mutant
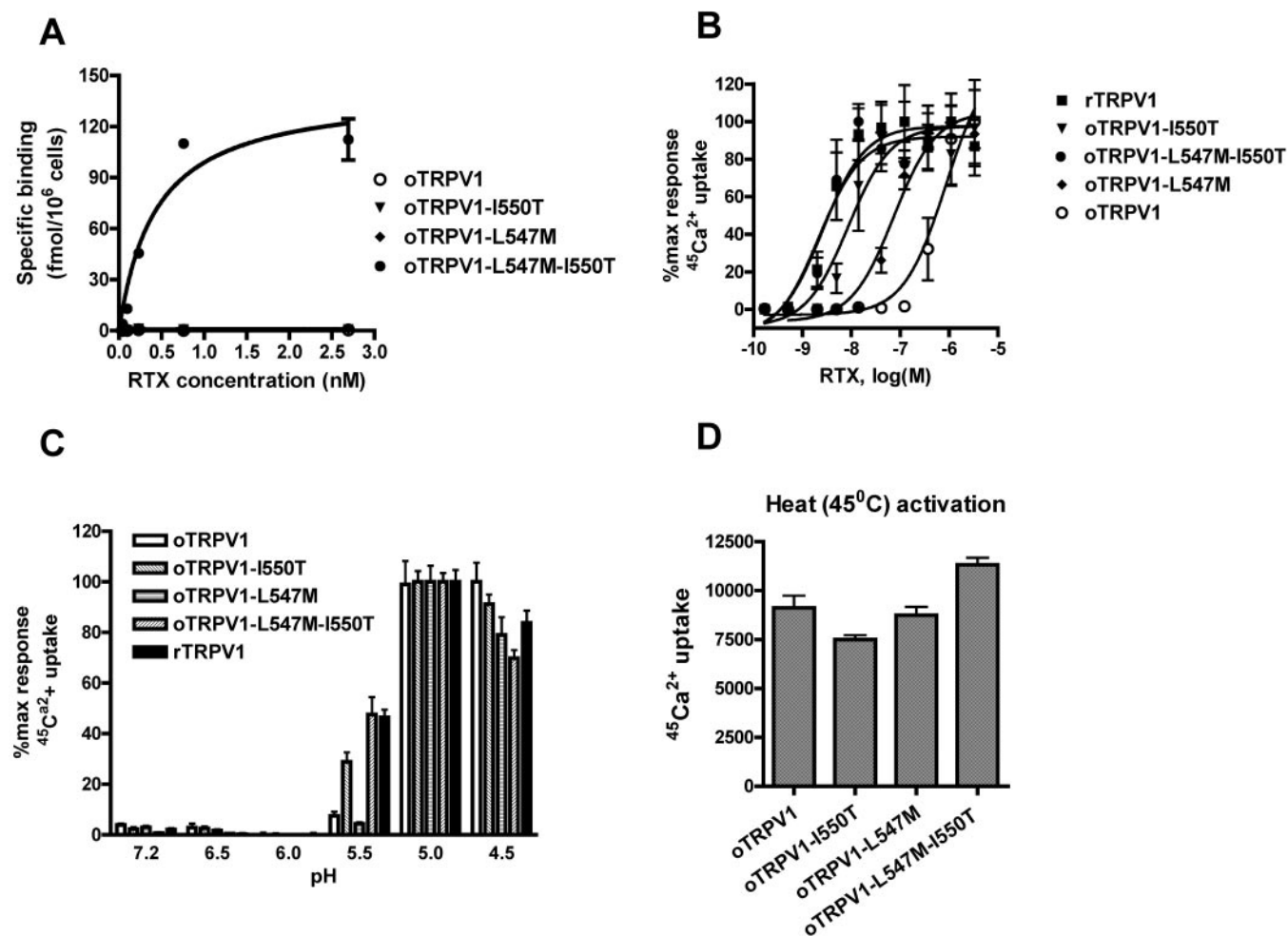
FIG. 5. **Both Met[547] and Thr[550] are required for measurable specific [³H]RTX binding.** CHO cells stably expressing TRPV1 were used. Each experiment was repeated twice in triplicate with similar results; *error bars* represent S.E. *A*, specific binding of [³H]RTX to wild type oTRPV1, oTRPV1-I550T, oTRPV1-L547M, or oTRPV1-L547M/I550T; the double mutant-expressing cells show saturable and specific binding of [³H]RTX (K_D value of 0.212 ± 0.09 nM). *B*, concentration-dependent stimulation of ${}^{45}Ca^{2+}$ uptake into cells expressing rTRPV1, oTRPV1, and oTRPV1 mutants by RTX. EC_{50} values are shown in Table II. *C*, stimulation of ${}^{45}Ca^{2+}$ uptake into cells expressing rTRPV1, oTRPV1, and oTRPV1 mutants by protons (pH range 4.5–7.2). Maximum response for each cell line was considered 100%. The rest were expressed as percentage of their maximum. *D*, stimulation of ${}^{45}Ca^{2+}$ uptake into cells expressing oTRPV1 and oTRPV1 mutants by heat (45 °C).

showed an increase in sensitivity to RTX but not to capsaicin in the functional ${}^{45}Ca^{2+}$-uptake assay, whereas a single I550T mutation resulted in gain of oTRPV1 sensitivity to both vanilloids. However, we were unable to measure [³H]RTX specific binding in cells expressing either one of these single mutants (Fig. 3*D*, 4*C*, and 5*A*). Therefore, we hypothesized that oTRPV1 might require both Thr[550] and Met[547] to attain measurable [³H]RTX binding. We constructed the oTRPV1 L547M/I550T double mutant and tested its vanilloid sensitivity in functional ${}^{45}Ca^{2+}$-uptake and [³H]RTX binding assays. As predicted, oTRPV1-L547M/I550T showed strong [³H]RTX binding with a K_D value of 0.212 ± 0.09 nM (Fig. 5*A*), along with only a slight increase in functional sensitivity to capsaicin and a somewhat greater increase for RTX, with EC_{50} values of 0.021 ± 0.01 μM and 2.2 ± 1 nM, respectively (Fig. 5*B* and Table II). This demonstrates that Met[547] and Thr[550], as present in native rTRPV1, are required for measurable [³H]RTX binding in oTRPV1.

None of the oTRPV1 gain of function mutations (I550T, L547M, and L547M/I550T) displayed significantly altered responses to protons or heat compared with native oTRPV1 (Fig. 5, *C* and *D*). In agreement with previous literature reports, rTRPV1 was activated by pH 5.5 and below. oTRPV1 showed strong activation at pH 5 and below, slightly different from rat TRPV1. Changing the residues in oTRPV1 to the corresponding

residues in rTRPV1 (I550T and L547M/I550T) resulted in a slight change in sensitivity to pH 5.5. Heat (45 °C)-induced ${}^{45}Ca^{2+}$ uptake by oTRPV1 gain-of-function mutants did not demonstrate any significant variations from that of the wild type channel (Fig. 5*D*). These results verify that oTRPV1 and the various mutant proteins were expressed and were able to integrate multiple noxious stimuli despite their differential sensitivity to vanilloids.

Gain of Capsaicin Sensitivity Parallels Sensitivity to Other Agonists—We have measured ${}^{45}Ca^{2+}$ uptake by oTRPV1-transfected cells in response to a variety of TRPV1 agonists, including the vanilloids RTX, capsaicin, olvanil, arvanil, and PPAHV as well as the proposed endogenous ligands, NADA and OLDA. Although binding of [³H]RTX was not detectable, RTX did activate oTRPV1 with an EC_{50} of 655 ± 50 nM in the ${}^{45}Ca^{2+}$ uptake assay compared with 3 ± 0.1 nM EC_{50} of rTRPV1 (Table II). Arvanil, olvanil, NADA, OLDA, AEA, and PPAHV showed no agonist activity at oTRPV1 up to 40 μM under physiological pH conditions (pH 7.2), although they did activate rTRPV1. The rank order of agonist potency for rTRPV1 was RTX > olvanil > capsaicin > arvanil > PPAHV > NADA > OLDA (Table II). Gain of capsaicin and RTX sensitivity by oTRPV1-I550T and L547M/I550T mutants was paralleled with their gain of sensitivity to other TRPV1 agonists (RTX, olvanil, capsaicin, arvanil, NADA, OLDA). The rank order of potency for

TABLE III
Inhibition of capsaicin and proton induced activation of TRPV1

Selected antagonists were tested in CHO cells stably expressing rTRPV1, oTRPV1, oTRPV1-L547M, oTRPV1-I550T, or oTRPV1-L547M/I550M. Cells were activated by 0.5 μM capsaicin or pH 5.0. IC_{50} value for each antagonist was determined using Prism software and is expressed in micromolar.

TRPV1 or mutant	Ruthenium red	Capsazepine	BCTC	Iodo-RTX
Antagonist IC_{50} value in μM at pH 5 activation				
oTRPV1	2.397 ± 0.64	>40	>0.4	>0.4
oTRPV1-L547M	1.15 ± 0.14	>40	>0.4	N/A
oTRPV1-I550T	1.383 ± 0.465	0.079 ± 0.024	0.0044 ± 0.0009	0.004 ± 0.0003
oTRPV1-L547M/I550T	2.686 ± 0.487	>40	0.0042 ± 0.0027	0.014 ± 0.0017
rTRPV1	1.441 ± 0.044	>40	0.0006 ± 0.0005	0.029 ± 0.006
hTRPV1	0.94 ± 0.22	0.069 ± 0.01	0.0007 ± 0.0002	0.015 ± 0.002
Antagonist IC_{50} value in μM at capsaicin activation				
oTRPV1-I550T	1.162 ± 0.25	0.207 ± 0.141	0.0024 ± 0.0016	0.003 ± 0.0005
oTRPV1-L547M/I550T	1.084 ± 0.071	0.680 ± 0.522	0.001 ± 0.0008	0.0036 ± 0.0006
rTRPV1	1.021 ± 0.365	0.987 ± 0.401	0.0005 ± 0.0001	0.0038 ± 0.0002
hTRPV1	1.37 ± 0.29	0.053 ± 0.035	0.0003 ± 0.0001	0.004 ± 0.001

vanilloids at sensitive oTRPV1 mutants was RTX > olvanil $\geq$ arvanil > capsaicin > NADA > OLDA (Table II).

Of note, PPAHV (a full agonist at rat but not human TRPV1 (18)) requires a double mutation of L547M/I550T in oTRPV1 for agonist activity to be observed (Table II). oTRPV1-I550T is similar to hTRPV1 (Leu[547]), and no activation by PPAHV is seen, whereas oTRPV1-L547M/I550T is similar to rTRPV1 (Met[547]), and activation is detected, indicating that PPAHV agonism requires both Met[547] and Thr[550]. This suggests that Met[547] is an important determinant for RTX and RTX-like molecules, which also points out the differences between capsaicinoid and resiniferanoid-like molecules.

Vanilloid Sensitivity Also Confers Competitive Antagonism—To further explore the pharmacology of oTRPV1 and its vanilloid-sensitive mutants we have looked at the ability of a number of different antagonists to block various modes of activation of these channels. A Ca^{2+} channel pore blocker Ruthenium Red blocked pH 5 and capsaicin activation of rTRPV1, hTRPV1, oTRPV1, oTRPV1-I550T, and oTRPV1-L547M/I550T with IC_{50} values of ~ 1 μM (Table III). Because oTRPV1 is not sensitive to capsaicin and oTRPV1-I550T and oTRPV1-L547M/I550T mutants are, we were curious to see if recently reported TRPV1 antagonists inhibit proton activation of wild type oTRPV1, as well as proton and capsaicin activation of its mutants. We chose antagonists that were reported to block both capsaicin and proton activation of human and rat TRPV1, *i.e.* BCTC and Iodo-RTX (29–31) as well as capsazepine, reported to block human, but not rat TRPV1 responses to low pH (18).

As in previous reports, BCTC and Iodo-RTX were potent antagonists of rTRPV1 and hTRPV1 activated by capsaicin (IC_{50} values for BCTC at rTRPV1, 0.5 ± 0.1 nM, at hTRPV1, 0.3 ± 0.1 nM, and Iodo-RTX at rTRPV1, 3.8 ± 0.2 nM, at hTRPV1, 4 ± 1 nM), as well as by protons (pH 5.0 IC_{50} values for BCTC and Iodo-RTX at rTRPV1 are 0.6 ± 0.5 nM and 29 ± 6 nM, respectively; at hTRPV1 they are 0.7 ± 0.2 nM and 15 ± 2 nM, respectively). However, neither of the above mentioned antagonists (up to 0.4 μM, more than 100-fold the rTRPV1 IC_{50}) inhibited proton activation of oTRPV1, further demonstrating that oTRPV1 lacks the key determinants for binding of competitive antagonists such as BCTC and Iodo-RTX (Fig. 6 and Table II).

We hypothesized that compounds capable of antagonizing capsaicin and proton activation of rTRPV1 might also antagonize capsaicin and proton activation of vanilloid-sensitive oTRPV1-I550T and L547M/I550T mutants. As predicted, BCTC and Iodo-RTX both inhibited $^{45}Ca^{2+}$ uptake mediated by oTRPV1-I550T and oTRPV1-L547M/I550T in response to capsaicin or proton activation. BCTC and Iodo-RTX inhibited capsaicin activation of oTRPV1-I550T with IC_{50} values of 2.4 ± 1.6

nM and 3.0 ± 0.5 nM, respectively, and of oTRPV1-L547M/I550T with IC_{50} values of 1.0 ± 0.8 nM and 3.6 ± 0.6 nM, respectively (Table III). BCTC inhibited proton activation of oTRPV1-I550T with an IC_{50} value of 4.4 ± 0.9 nM and oTRPV1-L547M/I550T with an IC_{50} value of 4.2 ± 2.7 nM (Fig. 6 and Table III). Iodo-RTX inhibited proton activation of the oTRPV1-I550T mutant with an IC_{50} value of 4.0 ± 0.3 nM and oTRPV1-L547M/I550T with an IC_{50} value of 14 ± 1.7 nM (Table III). In summary, BCTC and Iodo-RTX IC_{50} values were similar for rat, human, and vanilloid-sensitive mutants of rabbit TRPV1 activated with capsaicin or proton. These results clearly demonstrate that Thr[550] is not only critical for vanilloid agonist sensitivity but also for the ability of competitive antagonists to block various modes of TRPV1 channel activation.

Although capsazepine antagonism of capsaicin was similar at rat, human, and vanilloid-sensitive oTRPV1 mutants (I550T, L547M/I550T), its antagonism of proton (pH 5) activation indicated an interesting pharmacological difference. Presence of Leu[547] seems to be essential with regard to capsazepine antagonism at proton activation. IC_{50} values for capsazepine were similar at proton activated oTRPV1-I550T and hTRPV1 (0.079 ± 0.024 and 0.069 ± 0.01 μM, respectively, Table III), but capsazepine was inactive up to 40 μM against proton activated oTRPV1-L547M/I550T and native rTRPV1. Both oTRPV1-I550T and hTRPV1 have leucine at position 547, whereas oTRPV1-L547M/I550T and rTRPV1 have methionine. Based on these results we propose that Leu[547] is required for capsazepine antagonism of proton activation of TRPV1, although it is possible that additional residues common to human and rabbit TRPV1 within Ser[505]-Thr[550] region (Met[514], Ala[525], Thr[526], and His[533]) might also contribute to capsazepine antagonism of proton activated TRPV1.

DISCUSSION

It has been reported that membranes derived from rabbit dorsal root ganglia (DRG) lack [³H]RTX binding in contrast to many species. In an attempt to determine the structural requirements for agonism and antagonism of TRPV1, we cloned and characterized a cDNA from a rabbit DRG cDNA library. The cDNA reported here appears to be an orthologue of human TRPV1. oTRPV1 mRNA is highly expressed in rabbit dorsal root ganglia and appears to be localized primarily to the small to medium size cell bodies similar to published observations on both rat and human TRPV1. Furthermore, oTRPV1 expressed heterologously in CHO or HEK293 cells can be activated by the expected physical stimuli (protons and heat) similar to rat and human TRPV1. However, as expected from the [³H]RTX binding studies, oTRPV1 is relatively insensitive to vanilloid ago-
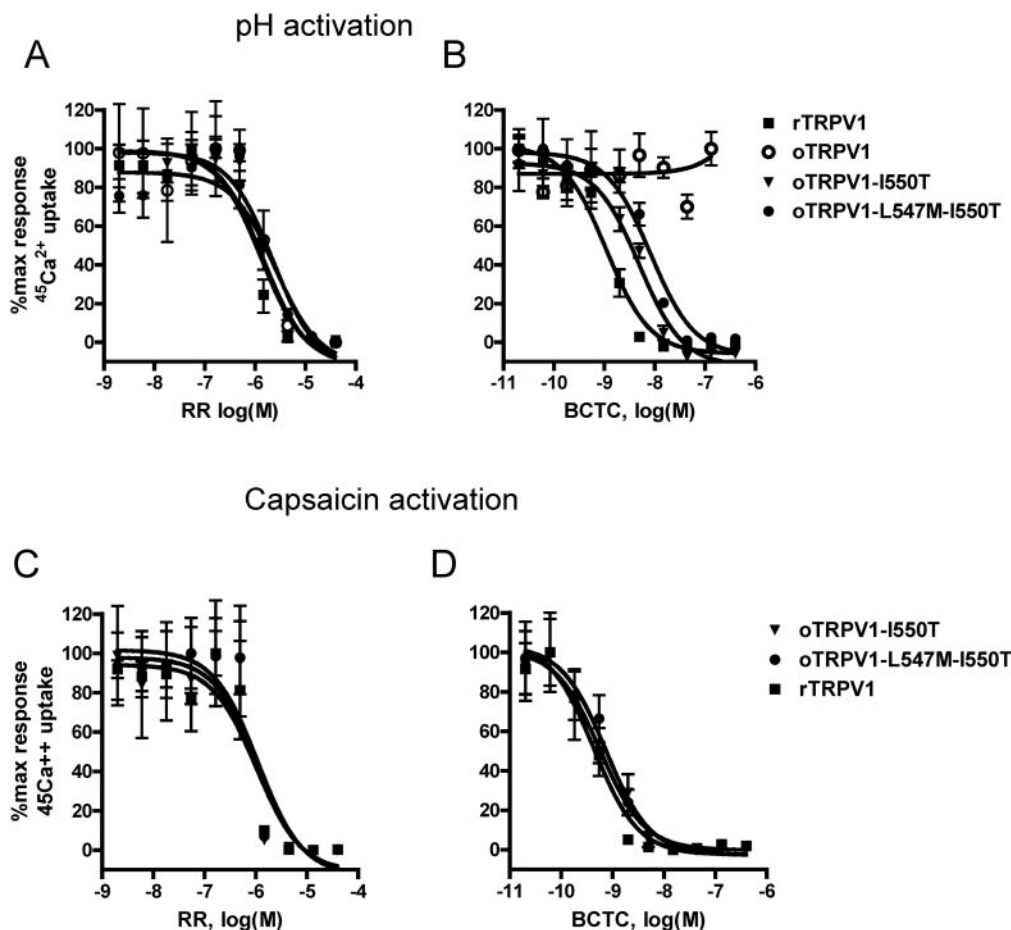
FIG. 6. **TRPV1 sensitivity to vanilloids also confers competitive antagonism.** Comparison of antagonists for inhibition of $^{45}Ca^{2+}$ uptake induced by protons and RTX. CHO cells stably expressing rTRPV1, oTRPV1, and mutants were seeded and assayed as described under "Experimental Procedures." $^{45}Ca^{2+}$ uptake was induced by pH 5 (*A* and *B*) or 0.5 μM capsaicin (*C* and *D*), in the presence of indicated concentrations of the antagonists. All experiments were repeated at least two times with similar results. *Points* represent mean values of triplicate determinations in single representative experiments; *error bars* represent S.E. IC$_{50}$ values are shown in Table III.

nists (RTX, capsaicin, arvanil, and olvanil; Table II) as compared with rat and human TRPV1.

Analogous to the published observations of Jordt and Julius (15) in gTRPV1, substitution of the TM3 to TM4 region (Ser[505]-Thr[550]) from rat or human TRPV1 confers vanilloid sensitivity to oTRPV1 equivalent to the wild type rat and human TRPV1 receptors, as measured by calcium uptake assays and whole cell electrophysiology studies. Jordt and Julius further demonstrated that residue 511, a tyrosine, was critical for vanilloid sensitivity. Our observations agree with those of Jordt and Julius, however, because Tyr[511] is a conserved residue across species, it cannot explain the differences we have observed in vanilloid sensitivity in rabbit TRPV1 and other species. Comparison of the sequence in the TM3–TM4 domain across species identified candidate residues potentially underlying the pharmacological differences. Single point mutations of the rabbit TRPV1 channel were prepared, by substituting residues from the rat TRPV1 channel, and the hybrid channels were functionally characterized. These studies have resulted in the identification of two novel residues, which confer vanilloid sensitivity and high affinity [³H]RTX binding in rabbit, rat, and human TRPV1 channels. Remarkably, we demonstrate that oTRPV1 can gain functional vanilloid sensitivity with a single residue substitution (I550T), and furthermore we show that with one additional residue change (L547M), oTRPV1 also gains high affinity [³H]RTX binding. Indeed, reverse mutation of the rat and human residues at positions 550 and 547 show loss of vanilloid sensitivity and/or RTX binding.

Based on chimeric and mutagenesis studies on TRPV1 (Ref. 15 and the present study), vanilloid sensitivity and RTX binding are transferable with the TM3/4 region (Ser[505]-Thr[550]) from rat TRPV1 to chicken and rabbit orthologues as well as to other TRP family members such as TRPV2 and TRPV4. This favors that the vanilloid-binding site is defined by the TM3/4 region. This is further supported by the study of Jordt and Julius (15), in which they showed that a cysteine reactive reagent reversibly inhibited [³H]RTX binding to the rTRPV1 mutant, S512C, in the TM3/4 region, and the present study showing the gain of [³H]RTX binding by oTRPV1 double mutant L547M and I550T. In all, these results favor the hypothesis that Tyr[511], Met[547], and Thr[550] may be present in the binding pocket and are important molecular determinants for vanilloid sensitivity.

Based on these results models could be proposed showing capsaicin or RTX interacting with Tyr[511] and Thr[550]. Jordt and Julius (15) predicted that the aromatic portion of Tyr[511] interacts with the vanilloid moiety of capsaicin (aromatic-aromatic interaction). Although their model accounts for the charged capsaicin analogue (DA-5018.HCl) studies that indicated DA-5018.HCl interaction with the TRPV1 from intracellular side (20), an alternative model could be proposed by having vanilloid moiety interaction with Thr[550] and the "tail end" hydrophobic group of capsaicin or RTX interacting with Tyr[511] (Fig. 7). Thus, in the present model, Tyr[511] engages in hydrophobic interaction and partly accounts for the observed differences in affinity between ligands owing to the differences in the hydrophobic tails of these molecules, *i.e.* molecules with short ali-
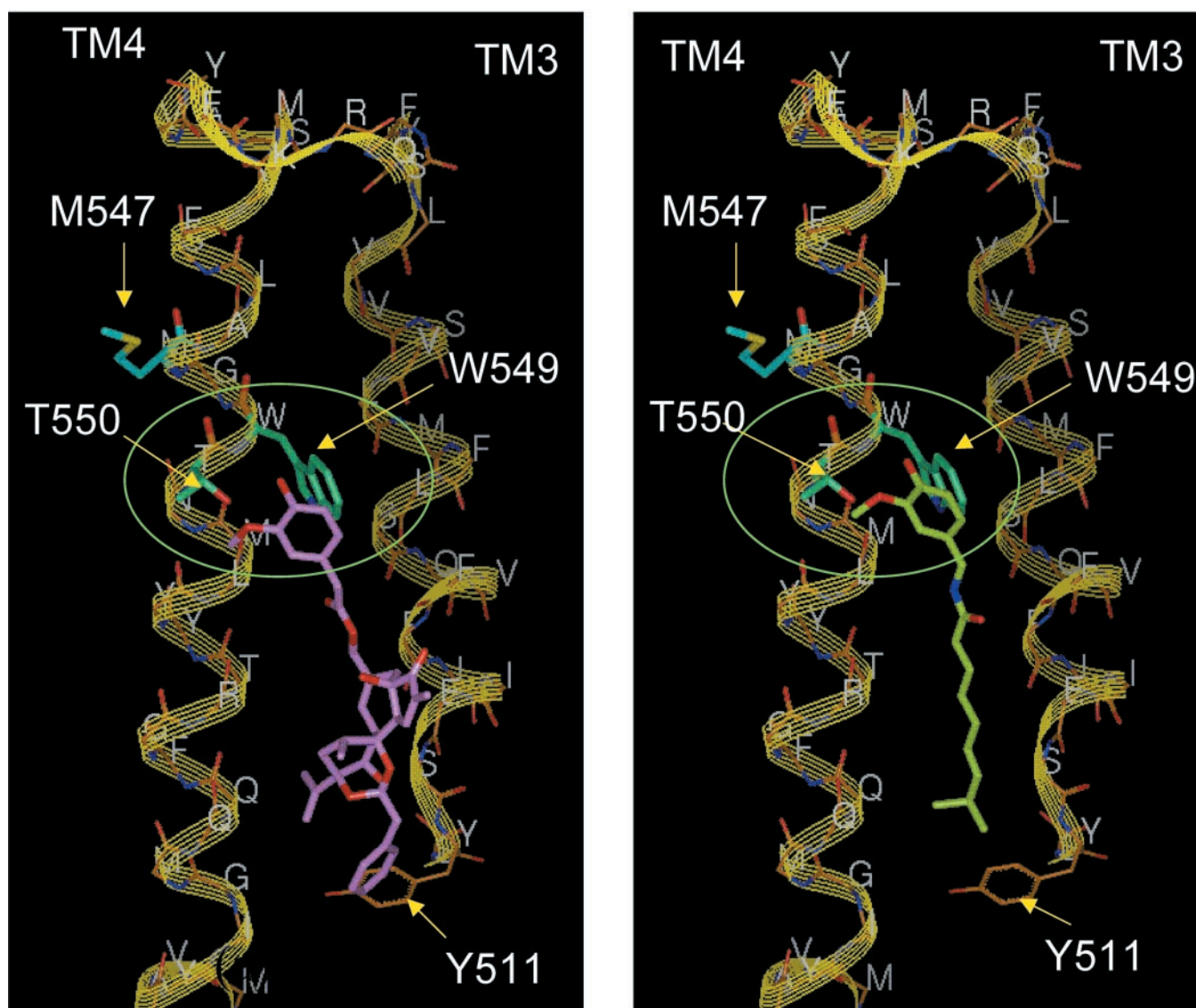
FIG. 7. **Structural model of RTX (*A*) and capsaicin (*B*) interacting with transmembrane helices TM3 and TM4 of TRPV1.** The backbone of the complete structural model along with the side chains of residues considered to be involved in interactions is shown. The side chains of Met[547], Trp[549], and Thr[550] are shown as *sticks (thick lines)*. Indicated interactions of vanillyl moiety with Thr[550] and Trp[549] are highlighted in the *green ellipses*. Residues considered to be involved in interactions with the substituted phenyl portions of the two ligands are shown in *cyan*. Modeled hydrophobic contacts of Tyr[511] with the hydrophobic ends of RTX and capsaicin are shown. RTX and capsaicin are shown in *pink* (*A*) and *green* (*B*), respectively.

phatic chain such as zingerone may not interact well with Tyr[511] and hence are weak agonists of TRPV1. On the other hand, molecules with long aliphatic chains such as arvanil and olvanil may interact with Tyr[511], and other hydrophobic side chains accounts for their strong agonist activity. Vanillyl moiety (methoxyphenol) is common for capsaicin, RTX, arvanil, olvanil, and zingerone; it is reasonable to assume that this part interacts with side-chain hydroxyl group of Thr[550]. Notably, the sensitivities observed by mutating residue 550 are consistent with the structure-activity relationship resulting from chemical modifications of the vanilloid moiety. For instance, mutational studies of oTRPV1 showed the gain of function by I550T and I550S, little change by I550C and I550A. Noting that Thr and Ser have the H-bonding-capable hydroxyl group, whereas Ala and Cys are similar in size but lack the H-bonding functional side-chain group, which is critical for agonist and antagonist activity. Correspondingly, capsaicin analogues with

minor modifications of hydroxyl and methoxyl, which reduce H-bonding potential, display weaker agonist (33) and antagonist activities.

In both models, Tyr[511] belongs to the transition between an intracellular loop and TM3, and residues Met[547] and Thr[550] belong to TM4. Based on the crystal structure of the K$^+$ channel and the derived "paddle" model of the TM3/4 region (34), it is possible that TM3/4 regions of the ion channels such as TRPV1 may form a paddle and the binding site near Thr[550] may not be as buried as the simple "straight up and down" helices imply. Thus, molecules with a charged group attached to the vanilloid moiety (such as DA-5018.HCl) may exhibit activity from intracellular side. Our model is dependent on further studies that evaluate the equivalence of ion selectivity, desensitization properties, and the paddle formation by the TM3/4 region of TRPV1, which will be important for validating our assumptions. Hence, interactions depicted in Fig. 7 have to

be interpreted only qualitatively but not in precise geometric terms. The current model and the model by Jordt and Julius (15) does not account for why N- and C-terminal domains of TRPV1 (24) or point mutations at Arg^{114} and Glu^{761} (23) result in loss of sensitivity to capsaicin and a concomitant loss of binding to [³H]RTX. Both models emphasize that residues in TM3/4 regions are critical for ligand recognition and assume that others in the N and C terminus play a modulatory role. These models are preliminary and require additional biochemical and structural information for validation and refinement of precise ligand orientation in the binding site.

Because there is no direct evidence that Tyr^{511}, Met^{547}, or Thr^{550} interact with the vanilloid moiety as might be shown either by chemical cross-linking of these residues with the vanilloid moiety or by a solved crystal structure of capsaicin or RTX bound to TRPV1, an alternate model based on conformational change could be proposed to explain our findings. In this alternative model, Thr^{550} and Met^{547} simply change the conformation of TRPV1 in a way that creates an optimal vanilloid binding site in the TM3/4 region that may include Tyr^{511}. However, this alternate model does not explain the structure-activity relationship resulting from modifications of the vanilloid moiety (33); hence, we do not favor the conformation change model.

In rabbit TRPV1, mutation of Leu^{547} to the corresponding rat Met^{547} resulted in a selective 30-fold higher sensitivity to RTX without a detectable increase in capsaicin sensitivity. RTX is essentially a vanilloid whose marked enhancement of potency, relative to capsaicin, is thought to be brought about by the resiniferanol moiety known as a C-region. The results of the L547M mutation in oTRPV1 imply that perhaps this residue contributes to a structural conformation that is favorable for interaction with RTX. Interestingly, the mutation of the rabbit TRPV1 Ile^{550} to Thr^{550} markedly enhanced the response to both capsaicin and RTX.

It has become clear from many studies that the measurement of binding to TRPV1, as determined by competition of [³H]RTX binding, and of calcium uptake reveals distinct structure activity relationships (28). TRPV1 is predominantly expressed at internal membranes in the cell, with only a small fraction at the plasma membrane where it can regulate calcium influx. An attractive explanation for the disparity in structure-activity relationships is that the TRPV1 channels present internally are different from those at the plasma membrane, presumably reflecting its differential modulation, whether by phosphorylation (35–37), interaction with phosphatidylinositol 1,4,5-bisphosphate (38), subunit conformation or association with other proteins (39). Pharmacological evidence for this assumption was the identification of a vanilloid antagonist that competitively blocked $^{45}Ca^{2+}$ uptake in response to capsaicin or RTX with high potency (K_i of ~100 nM) but which inhibited [³H]RTX binding less than 10% at 30 μM (29). This antagonist likewise was unable to block the release of calcium from internal stores by RTX. The mutational studies presented here complement such pharmacological observations, showing once again partial uncoupling between the assays for $^{45}Ca^{2+}$ uptake and [³H]RTX binding. In the present case, however, the differential selectivity is brought about by changes in the receptor rather than in the ligand. Thus, we find in the [³H]RTX binding assay that mutation of rat TRPV1 from either Met^{547} to Leu^{547} or Thr^{550} to Ile^{550} caused a reduction in binding affinity but not a change in potency for calcium uptake. Contribution of Met^{547} to higher affinity for [³H]RTX binding is consistent with the observation that human TRPV1, which lacks Met^{547}, has about 25-fold lower affinity for [³H]RTX binding compared with rTRPV1 (28).

We also studied the properties of several published antagonists, of the native and heterologous TRPV1 channels, to the known activators. We and others (30, 32) have shown that BCTC and Iodo-RTX are potent antagonists of capsaicin and proton activation of rat and human TRPV1. However, BCTC and Iodo-RTX are ineffective antagonists of oTRPV1 responses to protons (pH 5). Because BCTC and Iodo-RTX are in fact potent antagonists of oTRPV1 gain of function mutants (I550T and L547M/I550T), we believe that Thr^{550} is also a critical determinant for competitive antagonist binding. We speculate that Iodo-RTX could inhibit TRPV1 via an additional hydrophobic interaction involving the Iodo group. Overlay of capsazepine with the binding model of capsaicin shows that the polar dihydroxy phenyl part of the former will have similar interactions as the vanillyl moiety of the latter.

Clearly, the ability of capsaicin-site antagonists to block all modes of TRPV1 activation and identification of some of the key molecular determinants (Tyr^{511}, Met^{547}, and Thr^{550}) confirm this site as a key regulatory site on TRPV1 and may help in designing new antagonists with predictable structure-activity relationship. Given reports of the involvement of TRPV1 in inflammatory pain and other sensory neuronal disorders (8, 9), antagonists of hTRPV1 may prove useful in the treatment of human diseases such as arthritis, bladder cystitis, and irritable bowel syndrome.

REFERENCES

1. Caterina, M. J., Schumacher, M. A., Tominaga, M., Rosen, T. A., Levine, J. D., and Julius, D. (1997) *Nature* **389,** 816–824
2. Julius, D., and Basbaum, A. I. (2001) *Nature* **413,** 203–210
3. Clapham, D. E., Runnels, L. W., and Strubing, C. (2001) *Nat. Rev. Neurosci.* **6,** 387–396
4. Hwang, S. W., Cho, H., Kwak, J., Lee, S. Y., Kang, C. J., Jung, J., Cho, S., Min, K. H., Suh, Y. G., Kim, D., and Oh, U. (2000) *Proc. Natl. Acad. Sci. U. S. A.* **97,** 6155–6160
5. Olah, Z., Karai, L., and Iadarola, M. J. (2001) *J. Biol. Chem.* **276,** 31163–31170
6. Huang, S. M., Bisogno, T., Trevisani, M., Al-Hayani, A., De Petrocellis, L., Fezza, F., Tognetto, M., Petros, T. J., Krey, J. F., Chu, C. J., Miller, J. D., Davies, S. N., Geppetti, P., Walker, J. M., and Di Marzo V. (2002) *Proc. Natl. Acad. Sci. U. S. A.* **99,** 8400–8405
7. Chu, C. J., Huang, S. M., De Petrocellis, L., Bisogno, T., Ewing, S. A., Miller, J. D., Zipkin, R. E., Daddario, N., Appendino, G., Di Marzo, V., and Walker, J. M. (2003) *J. Biol. Chem.* **278,** 13633–13639
8. Ji, R. R., Samad, T. A., Jin, S. X., Schmoll, R., and Woolf, C. J. (2002) *Neuron* **36,** 57–68
9. Caterina, M. J., Leffler, A., Malmberg, A. B., Martin, W. J., Trafton, J., Petersen-Zeitz, K. R., Koltzenburg, M., Basbaum, A. I., and Julius, D. (2000) *Science* **288,** 306–313
10. Szallasi, A., and Blumberg, P. M. (1993) *Naunyn-Schmiedeberg's Arch. Pharmacol.* **347,** 84–91
11. Glinsukon, T., Stitmunnaithum, V., Toskulkao, C., Baranawuti, T., and Tangkrisanavinont, V. (1980) *Toxicon* **18,** 215–220
12. Hayes, P., Meadows, H. J., Gunthorpe, M. J., Harries, M. H., Duckworth, D. M., Cairns, W., Harrison, D. C., Clarke, C. E., Ellington, K., Prinjha, R. K., Barton, A. J., Medhurst, A. D., Smith, G. D., Topp, S., Murdock, P., Sanger, G. J., Terrett, J., Jenkins, O., Benham, C. D., Randall, A. D., Gloger, I. S., and Davis, J. B. (2000) *Pain* **88,** 205–215
13. Edenson, S., Tamir, R., Neering, S., Wild, K., Yang, R., Treanor, J., and Lile, J. (2000) *Soc. Neurosci. Abstr.* **26,** 39.4
14. Qu, Y., Klionsky, L., Tamir, R., Edenson, S., Wang, J., Lile, J., Wild, K., Gavva, N. R., and Treanor, J., (2003) *Biophys. J.* **84,** (suppl.) 434
15. Jordt, S. E., and Julius, D. (2002) *Cell* **108,** 421–430
16. Savidge, J., Davis, C., Shah, K., Colley, S., Phillips, E., Ranasinghe, S., Winter, J., Kotsonis, P., Rang, H., and McIntyre, P. (2002) *Neuropharmacology* **43,** 450–456
17. Szallasi, A., Blumberg, P. M., Annicelli, L. L., Krause, J. E., and Cortright, D. N. (1999) *Mol. Pharmacol.* **56,** 581–587
18. McIntyre, P., McLatchie, L. M., Chambers, A., Phillips, E., Clarke, M., Savidge, J., Toms, C., Peacock, M., Shah, K., Winter, J., Weerasakera, N., Webb, M., Rang, H. P., Bevan, S., and James, I. F. (2001) *Br. J. Pharmacol.* **132,** 1084–1094
19. Shin, J. S., Wang, M. H., Hwang, S. W., Cho, H., Cho, S. Y., Kwon, M. J., Lee, S. Y., and Oh, U. (2001) *Neurosci. Lett.* **299,** 135–139
20. Jung, J., Hwang, S. W., Kwak, J., Lee, S.-Y., Kang, C. J., Kim, W. B., Kim, D., and Oh, U. (1999) *J. Neurosci.* **19,** 529–538
21. Jordt, S. E., Tominaga, M., and Julius, D. (2000) *Proc. Natl. Acad. Sci. U. S. A.* **97,** 8134–8139
22. Welch, J. M., Simon, S. A., and Reinhart, P. H. (2000) *Proc. Natl. Acad. Sci.*

U. S. A. **97,** 13889–13894

23. Jung, J., Lee, S.-Y., Hwang, S. W., Cho, H., Shin, J., Kang, Y. S., Kim, S., and Oh, U. (2002) *J. Biol. Chem.* **277,** 44448–44454

24. Vlachova, V., Teisinger, J., Suankova, K., Lyfenko, A., Ettrich, R., and Vyklicky, L. (2003) *J. Neurosci.* **23,** 1340–1350

25. Wilcox, J. N. (1993) *J. Histochem. Cytochem.* **41,** 1725–1733

26. Hamill, O. P., Marty, A., Neher, E., Sakmann, B., and Sigworth, F. J. (1981) *Pflugers Arch.* **391,** 85–100

27. Szallasi, A., and Blumberg, P. M. (1999) *Pharmacol. Rev.* **51,** 159–212

28. Acs, G., Lee, J., Marquez, V., and Blumberg, P. M. (1996) *Mol. Brain Res.* **35,** 173–182

29. Toth, A., Blumberg, P. M., Chen, Z., and Kozikowski, A. P. (2004) *Mol. Pharmacol.* **65,** 282–291

30. Valenzano, K. J., Grant, E. R., Wu, G., Hachicha, M., Schmid, L., Tafesse, L., Sun, Q., Rotshteyn, Y., Francis, J., Limberis, J. T., Malik, S., Whittemore, E. R., Hodges, D. D. (2003) *J. Pharmacol. Exp. Ther.* **306,** 377–386

31. Pomonis, J. D., Harrison, J. E., Mark, L., Bristol, D. R., Valenzano, K. J., and Walker, K. (2003) *J. Pharmacol. Exp. Ther.* **306,** 387–393

32. Wahl, P., Foged, C., Tullin, S., and Thomsen, C. (2001) *Mol. Pharmacol.* **59,** 9–15

33. Walpole, C. S., Wrigglesworth, R., Bevan, S., Campbell, E. A., Dray, A., James, I. F., Perkins, M. N., Reid, D. J., and Winter, J. (1993) *J. Med. Chem.* **36,** 2362–2372

34. Jiang, Y., Lee, A., Chen, J., Ruta, V., Cadene, M., Chait, B. T., and MacKinnon, R. (2003) *Nature* **423,** 33–41

35. Premkumar, L. S., and Ahern, G. P. (2000) *Nature* **408,** 985–990

36. Bhave, G., Zhu, W., Wang, H., Brasier, D. J., Oxford, G. S., and Gereau, R. W. 4th. (2002) *Neuron* **35,** 721–731

37. Numazaki, M., Tominaga, T., Toyooka, H., and Tominaga, M. (2002) *J. Biol. Chem.* **277,** 13375–13378

38. Prescott, E. D., and Julius, D. (2003) *Science* **300,** 1284–1288

39. Numazaki, M., Tominaga, T., Takeuchi, K., Murayama, N., Toyooka, H., and Tominaga, M. (2003) *Proc. Natl. Acad. Sci. U. S. A.* **100,** 8002–8006